Ain Shams Engineering Journal (2014) 5, 575–584

Ain Shams University

Ain Shams Engineering Journal

www.elsevier.com/locate/asej
www.sciencedirect.com

ENGINEERING PHYSICS AND MATHEMATICS

Entropy generation due to MHD flow in a porous channel with Navier slip

Sanatan Das [a], **Rabindra Nath Jana** [b,*]

[a] *Department of Mathematics, University of Gour Banga, Malda 732 103, India*
[b] *Department of Applied Mathematics, Vidyasagar University, Midnapore 721 102, India*

Received 21 August 2013; revised 15 October 2013; accepted 13 November 2013
Available online 28 December 2013

KEYWORDS
MHD flow;
Slip parameters;
Peclet number;
Brinkmann number;
Entropy generation number;
Bejan number

Abstract Effects of magnetic field and Navier slip on the entropy generation in a flow of viscous incompressible electrically conducting fluid between two infinite horizontal parallel porous plates under a constant pressure gradient have been studied. An exact solution of governing equation has been obtained in closed form. The entropy generation number and the Bejan number are also obtained. The influences of the pertinent flow parameters on velocity, temperature, entropy generation and Bejan number are discussed with the aid of graphs.

1. Introduction

The foundation of knowledge of entropy generation goes back to Clausius and Kelvins studies on the irreversibility aspects of the second law of thermodynamics. However, the entropy generation resulting from temperature differences has remained untreated by classical thermodynamics. The second law analysis is important because it is one of the methods used for predicting the performance of engineering processes. Since entropy generation is the measure of the destruction of available work of the system, the determination of the active factors motivating the entropy generation is important in upgrading the system performances. Rapid progress in science and technology has led to the development of an increasing number of flow devices that involve the manipulation of fluid flow in various geometries. Many textbooks of fluid dynamics fails to mention that the no-slip condition remains an assumption due to unusual agreement with experimental results for a century. Nevertheless, another approach supposed that fluid can slide over a solid surface because the experimental fact was not always accepted in the past. Navier [1] proposed general boundary conditions which include possibility of fluid slip at the solid boundary. He proposed that velocity at a solid surface is proportional to the shear stress at the surface. The phenomenon of slip occurrence has been demonstrated by the recent theoretical and experimental studies such as Sahraoui et al. [2], Buckingham et al. [3], Berh [4], Raoufpanah [5], Chauhan et al. [6], Tripathi et al. [7] and Gupta [8]. Moreover, entropy generation in engineering and industrial flow systems provides insight into the power consumption through thermodynamic losses. Therefore, the entropy minimization provides power optimization for the fluid motion in the porous channel. Efficient energy utilization during the convection in any fluid

* Corresponding author. Tel.: +91 3222261171.
E-mail addresses: tutusanasd@yahoo.co.in (S. Das), jana261171@yahoo.co.in (R.N. Jana).
Peer review under responsibility of Ain Shams University.

Production and hosting by Elsevier

2090-4479 © 2013 Production and hosting by Elsevier B.V. on behalf of Ain Shams University.
http://dx.doi.org/10.1016/j.asej.2013.11.005

flow is one of the fundamental problems of the engineering processes to improve the system.

The problem of the slip flow regime is very important in this era of modern science, technology and vast ranging industrialization. In many practical applications, the fluid adjacent to a solid surface no longer takes the velocity of the surface. The fluid at the surface has a finite tangential velocity; it slips along the surface. The flow regime is called the slip flow regime and its effect cannot be neglected. The effects of slip conditions on the hydromagnetic steady flow in a channel with permeable boundaries were discussed by Makinde and Osalusi [9]. Khalid and Vafai [10] obtained the closed form solutions for steady periodic and transient velocity field under slip condition. Watanebe et al. [11] studied the effect of Navier slip on Newtonian fluids at solid boundary. Chen and Tian [12] investigated entropy generation in a micro annulus flow and discussed the influence of velocity slip on entropy generation. Use of an external magnetic field is of considerable importance in many industrial applications, particularly as a control mechanism in material manufacturing. Homogeneity and quality of single crystals grown from doped semiconductor melts is of interest to manufacturers of electronic chips. One of the main purposes of electromagnetic control is to stabilize the flow and suppress oscillatory instabilities, which degrades the resulting crystal. The magnetic field strength is one of the most important factors for crystal formation. The scientific treatment of the problems of irrigation, soil erosion and tile drainage are the present focus of the development of porous channel flow. The magnetohydrodynamic channel flow with heat transfer has attracted the attention of many researchers due to its numerous engineering and industrial applications. Such flows finds applications in thermofluid transport modeling in magnetic geosystems, meteorology, turbo machinery, solidification process in metallurgy and in some astrophysical problems. One of the methods used for predicting the performance of the engineering processes is the second law analysis. The second law of thermodynamics is applied to investigate the irreversibilities in terms of the entropy generation rate. Since entropy generation is the measure of the destruction of the available work of the system, the determination of the factors responsible for the entropy generation is also important in upgrading the system performances. The method is introduced by Bejan [13,14]. The entropy generation is encountered in many energy-related applications, such as solar power collectors, geothermal energy systems and the cooling of modern electronic systems. Efficient utilization of energy is the primary objective in the design of any thermodynamic system. This can be achieved by minimizing entropy generation in processes. The theoretical method of entropy generation has been used in the specialized literature to treat external and internal irreversibilities. The irreversibility phenomena, which are expressed by entropy generation in a given system, are related to heat and mass transfers, viscous dissipation, magnetic field etc. Several researchers have discussed the irreversibility in a system under various flow configurations [15–26]. They showed that the pertinent flow parameters might be chosen in order to minimize entropy generation inside the system. Salas et al. [27] analytically showed a way of applying entropy generation analysis for modeling and optimization of magnetohydrodynamic induction devices. They restricted their analysis to only Hartmann model flow in a channel. Thermodynamics analysis of mixed convection in a channel with transverse hydromagnetic effect has been investigated by Mahmud et al. [28]. Flow, thermal and entropy generation characteristic inside a porous channel with viscous dissipation have been investigated by Mahmud [29]. The heat transfer and entropy generation during compressible fluid flow in a channel partially filled with porous medium have been analyzed by Chauhan and Kumar [30]. Tasnim et al. [31] have studied the entropy generation in a porous channel with hydromagnetic effects. Eegunjobi and Makinde [32] have studied the combined effect of buoyancy force and Navier slip on entropy generation in a vertical porous channel. The second law analysis of laminar flow in a channel filled with saturated porous media has been studied by Makinde and Osalusi [33]. Makinde and Maserumule [34] has presented the thermal criticality and entropy analysis for a variable viscosity Couette flow. Makinde and Osalusi [35] have investigated the entropy generation in a liquid film falling along an incline porous heated plate. Cimpean and Pop [36,37] have presented the parametric analysis of entropy generation in a channel. The effect of an external oriented magnetic field on entropy generation in natural convection has been investigated by Jery et al. [38]. Dwivedi et al. [39] have made an analysis on the incompressible viscous laminar flow through a channel filled with porous media. Analysis of entropy generation rate in an unsteady porous channel flow with Navier slip and convective cooling has been presented by Chinyoka and Makinde [40]. Chinyoka et al. [44] have presented the entropy analysis of unsteady magnetic flow through a porous pipe with buoyancy effects. The entropy regime for radiative MHD Couette flow inside a channel with naturally permeable base has been studied by Vyas and Rai [45].

In this paper, our objective is to investigate the combined effects of magnetic field, suction/injection and Navier slips on entropy generation in an MHD flow through a porous channel under a constant pressure gradient. Closed form solution has been obtained for the fluid velocity and the fluid temperature. A parametric study is carried out to see how the pertinent parameters of the problem affect the flow field, temperature field and the entropy generation.

2. Mathematical formulation and its solution

Consider the viscous incompressible electrically conducting fluid bounded by two infinite horizontal parallel porous plates separated by a distance h. Choose a cartesian co-ordinate

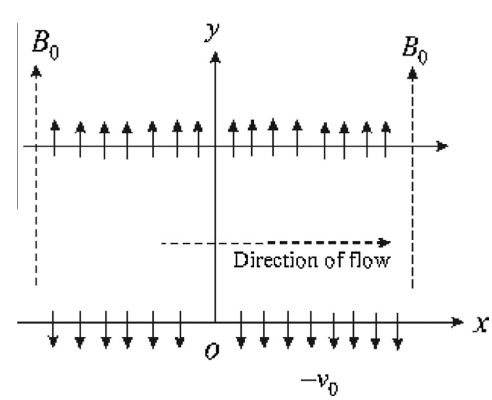

Figure 1 Geometry of the problem.

system with x-axis along the lower stationary plate in the direction of the flow, the y-axis is perpendicular to the plates (see Fig. 1). A uniform transverse magnetic field B_0 is applied perpendicular to the channel plates. Since the plates are infinitely long, all physical variables, except pressure, depend on y only. The equation of continuity then gives $v = -v_0$ everywhere in the fluid where v_0 is the suction velocity at the plates.

The equations of motion along x-direction is

$$-v_0 \frac{du}{dy} = -\frac{1}{\rho}\frac{\partial p}{\partial x} + \nu \frac{d^2 u}{dy^2} - \frac{\sigma B_0^2}{\rho} u, \tag{1}$$

where u is the fluid velocity in the x-axis, ρ is the fluid density, ν the kinematic viscosity, σ the electrical conductivity of the fluid and p is the fluid pressure.

The energy equation is

$$-v_0 \frac{dT}{dy} = \frac{k}{\rho c_p}\frac{d^2 T}{dy^2} + \frac{\mu}{\rho c_p}\left(\frac{du}{dy}\right)^2 + \lambda \frac{\sigma B_0^2}{\rho c_p} u^2, \tag{2}$$

where μ is the coefficient of viscosity, k the thermal conductivity, c_p the specific heat at constant pressure, the index λ in the Eq. (3) is set equal to 0 for excluding Jule dissipation and 1 for including Jule dissipation.

The boundary conditions are

$$\begin{aligned} u &= \gamma_1 \frac{du}{dy}, \quad T = T_0 \quad \text{at } y = 0, \\ u &= \gamma_2 \frac{du}{dy}, \quad T = T_h \quad \text{at } y = h, \end{aligned} \tag{3}$$

where T is the fluid temperature, T_h the temperature at upper plate, T_0 the temperature at the lower plate and γ_1 and γ_2 slip coefficients.

Introducing the non-dimensional variables

$$\eta = \frac{y}{h}, \quad u_1 = \frac{u}{v_0}, \quad \theta = \frac{T - T_0}{T_h - T_0}, \tag{4}$$

Eqs. (1) and (2) become

$$\frac{d^2 u_1}{d\eta^2} - Re\frac{du_1}{d\eta} - M^2 u_1 = -P, \tag{5}$$

$$\frac{d^2\theta}{d\eta^2} - Pe\frac{d\theta}{d\eta} + Br\left[\left(\frac{du_1}{d\eta}\right)^2 + \lambda M^2 u^2\right] = 0, \tag{6}$$

where $M^2 = \frac{\sigma B_0^2 h^2}{\rho \nu}$ is the magnetic parameter, $Br = \frac{\mu v_0^2}{k(T_h - T_0)}$ the Brinkmann number, $Pe = \frac{v_0 h \rho c_p}{k}$ the Peclet number, $Re = \frac{v_0 h}{\nu}$ the Reynolds number and $P = \frac{h^2}{\rho \nu v_0}\left(-\frac{\partial p}{\partial x}\right)$ the non-dimensional pressure gradient.

The boundary conditions for $u_1(\eta)$ and $\theta(\eta)$ are

$$\begin{aligned} u_1 &= \beta_1 \frac{du_1}{d\eta}, \quad \theta = 0 \quad \text{at } \eta = 0, \\ u_1 &= \beta_2 \frac{du_1}{d\eta}, \quad \theta = 1 \quad \text{at } \eta = 1, \end{aligned} \tag{7}$$

where $\beta_1 = \frac{\gamma_1}{h}$ and $\beta_2 = \frac{\gamma_2}{h}$ are the slip parameters.

The solution of the Eq. (5) subject to the boundary conditions (7) is

$$u_1(\eta) = \frac{P}{M^2} + (A\cosh n\eta + B\sinh n\eta)\, e^{\frac{Re}{2}\eta}, \tag{8}$$

where

$$n = \left(\frac{Re^2}{4} + M^2\right)^{\frac{1}{2}},$$

$$A = \frac{\frac{P}{M^2}\left[n\beta_1 e^{-\frac{Re}{2}} + \sinh n - \beta_2\left(\frac{Re}{2}\sinh n + n\cosh n\right)\right]}{n(\beta_1 - \beta_2)\cosh n + \left[\left(\frac{Re^2}{4} - n^2\right)\beta_1\beta_2 - \frac{1}{2}Re(\beta_1 + \beta_2) + 1\right]\sinh n}, \tag{9}$$

$$B = \frac{P}{n\beta_1 M^2} + \frac{A}{n}\left(\frac{1}{\beta_1} - \frac{1}{2}Re\right). \tag{10}$$

The solution given by the Eq. (8) exists for both $Re < 0$ (corresponding to $v_0 < 0$ for the blowing at the plates) and $Re > 0$ (corresponding to $v_0 > 0$ for the suction at the plates).

On the use of (8), the Eq. (6) becomes

$$\begin{aligned} \frac{d^2\theta}{d\eta^2} - Pe\frac{d\theta}{d\eta} = -Br\Bigg[e^{Re\eta}\left\{A_8 + \frac{1}{2}(A_4\cosh 2n\eta + A_5\sinh 2n\eta)\right\} \\ \times 2P\lambda e^{\frac{Re}{2}\eta}(A_6\cosh n\eta + A_7\sinh n\eta) + \frac{\lambda P^2}{M^2}\Bigg]. \end{aligned} \tag{11}$$

Solution of the Eq. (11) subject to boundary condition (7) is given by

$$\begin{aligned} \theta(\eta) = c_1 + c_2 e^{Pe\eta} - Br\Bigg[e^{Re\eta}\left\{A_8 + \frac{1}{2}(A_4\cosh 2n\eta + A_5\sinh 2n\eta)\right\} \\ + \lambda P e^{\frac{Re}{2}\eta}(A_6\cosh n\eta + A_7\sinh n\eta) - \frac{\lambda P^2}{PeM^2}\eta\Bigg], \end{aligned} \tag{12}$$

where

$$\begin{aligned} A_1 &= \frac{1}{2}\left[\left(\frac{1}{2}ReA + nB\right)^2 + \lambda M^2(A^2 + B^2) - \left(\frac{1}{2}ReB + nA\right)^2\right], \\ A_2 &= \frac{1}{2}\left[\left(\frac{1}{2}ReA + nB\right)^2 + \lambda M^2(A^2 + B^2) + \left(\frac{1}{2}ReB + nA\right)^2\right], \\ A_3 &= \left(\frac{1}{2}ReA + nB\right)\left(\frac{1}{2}ReB + nA\right) + \lambda M^2 AB, \\ X_1 &= (Re + 2n)(Re + 2n - Pe), \quad X_2 = (Re - 2n)(Re - 2n - Pe), \\ X_3 &= \left(\frac{1}{2}Re + n\right)\left(\frac{1}{2}Re + n - Pe\right), \quad X_4 = \left(\frac{1}{2}Re - n\right)\left(\frac{1}{2}Re - n - Pe\right), \\ A_4 &= \frac{1}{X_1}(A_2 + A_3) + \frac{1}{X_2}(A_2 - A_3), \quad A_5 = \frac{1}{X_1}(A_2 + A_3) - \frac{1}{X_2}(A_2 - A_3), \\ A_6 &= \frac{1}{X_3}(A + B) + \frac{1}{X_4}(A - B), \quad A_7 = \frac{1}{X_3}(A + B) - \frac{1}{X_4}(A - B), \\ A_8 &= \frac{1}{Re^2 - RePe}. \end{aligned} \tag{13}$$

3. Results and discussion

To study the effects of magnetic field and Reynolds number on the velocity field we have presented the non-dimensional velocity u_1 against η in Figs. 2–5 for several values of magnetic parameter M^2, Reynolds number Re, slip parameters β_1 and β_2 with $P = 1$. It is seen from Figs. 2 and 3 that the fluid velocity u_1 decreases with an increase in either magnetic parameter M^2 or Reynolds number Re. This can be attributed to the presence of Lorentz force acting as a resistance to the flow as expected. The larger values of the Reynolds number correspond to higher suction/injection strength and hence clearly decreases the fluid velocity as illustrated in Fig. 3. Figs. 4 and 5 shows that the fluid velocity u_1 increases with an increase in slip parameter β_1 while it decreases with an increase in slip parameter β_2. We have plotted the temperature distribution θ against η in Figs. 6–8 for several values of Brinkmann number Br, Reynolds number Re and Peclet number Pe. It is seen from Figs. 4–8 that the fluid temperature θ increases with an

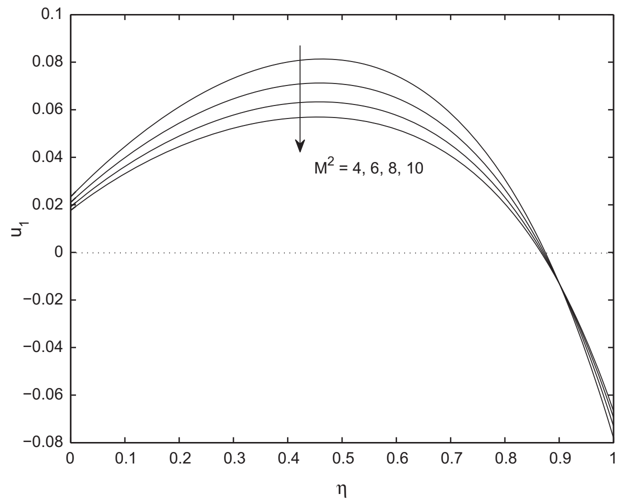

Figure 2 Velocity profiles for different M^2 when $Re = 2$, $\beta_1 = 0.1$ and $\beta_2 = 0.1$.

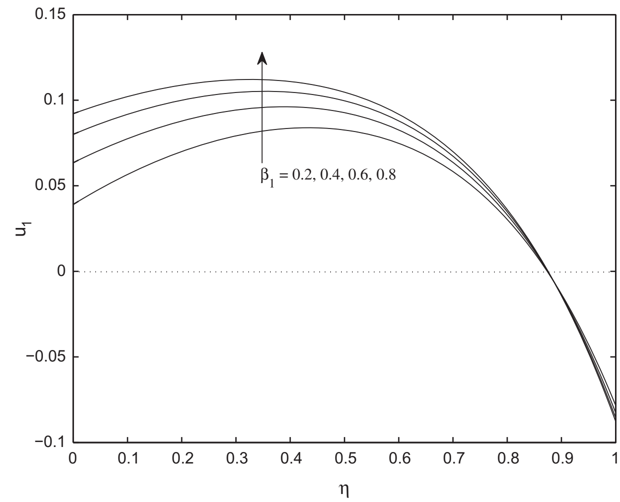

Figure 4 Velocity profiles for different β_1 when $Re = 0.5$, $M^2 = 5$ and $\beta_2 = 0.1$.

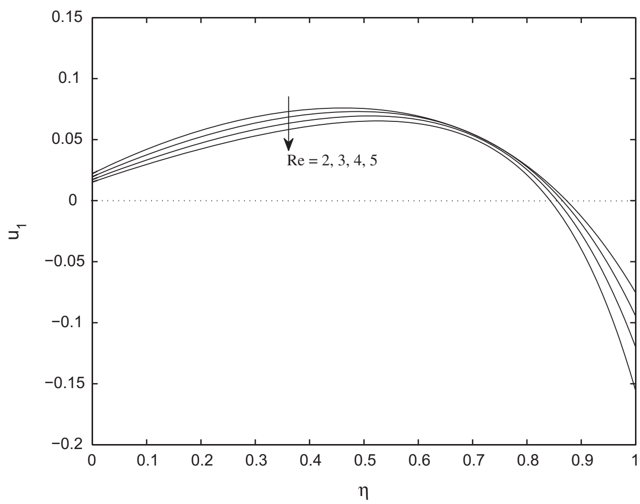

Figure 3 Velocity profiles for different Re when $M^2 = 5$, $\beta_1 = 0.1$ and $\beta_2 = 0.1$.

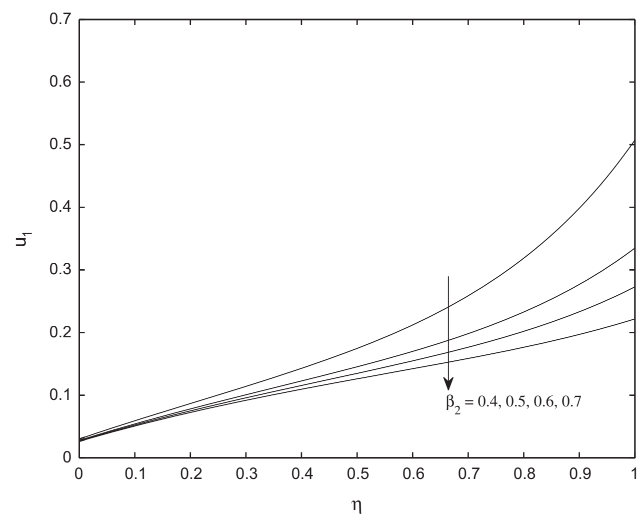

Figure 5 Velocity profiles for different β_2 when $M^2 = 5$, $\beta_1 = 0.1$ and $\beta_2 = 0.1$.

increase in either Brinkmann Br or Reynolds number Re or Peclet number Pe.

The rate of heat transfer at the plates $\eta = 0$ and $\eta = 1$ can be obtained from (12) as

$$\theta'(0) = c_2Pe - Br\Big[\Big\{ReA_8 + (ReA_4 + 2nA_5)\Big\} + \lambda P\left(\frac{1}{2}ReA_6 + nA_7\right) - \frac{\lambda P^2}{PeM^2}\Big], \tag{14}$$

$$\theta'(1) = c_2Pee^{Pe} - Br\big[e^{Re}\{A_1 + (ReA_4 + 2nA_5)\cosh 2n + (ReA_3 + 2nA_4)\sinh 2n\}P\lambda e^{\frac{Re}{2}}\Big\{\left(\frac{1}{2}ReA_6 + nA_7\right)\cosh n + \left(\frac{1}{2}ReA_7 + nA_6\right)\sinh n\Big\} - \frac{\lambda P^2}{PeM^2}\Big], \tag{15}$$

where A_1, A_2, A_3 and c_2 are given by (13).

The numerical values of the rate of heat transfers $\theta'(0)$ and $-\theta'(1)$ are entered in the Tables 1 and 2 for several values of M^2, Re, Br, Pe, β_1 and β_2. It is seen from the Table 1 that the rate of heat transfer $\theta'(0)$ at the plate $\eta = 0$ decreases with an increase in magnetic parameter M^2 whereas it increases with an increase in Reynolds number Re. The rate of heat transfer $-\theta'(1)$ at the plate $\eta = 1$ increases with an increase in magnetic parameter M^2 whereas it decreases with an increase in Reynolds number Re. Table 2 shows that the rate of heat transfer $\theta'(0)$ at the plate $\eta = 0$ decreases with an increase in Peclet number Pe whereas it increases with an increase in Brinkmann number Br. The rate of heat transfer $-\theta'(1)$ at the plate $\eta = 1$ increases with an increase in Peclet number Pe whereas it decreases with an increase in Brinkmann number Br. It is seen from the Table 3 that the rate of heat transfer $\theta'(0)$ at the plate $\eta = 0$ increases with an increase in slip parameter β_2 whereas it decreases with an increase in slip parameter β_1. The rate of heat transfer $-\theta'(1)$ at the plate $\eta = 1$ decreases with an increase in slip parameter β_2 whereas it increases with an increase in slip parameter β_1. On the other hand, $\theta'(1) < 0$ means the

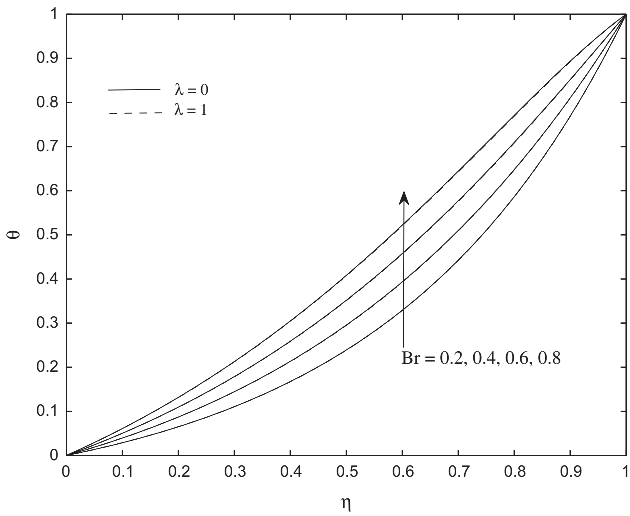

Figure 6 Temperature profiles for different *Br* when $Re = 2$ and $Pe = 3$.

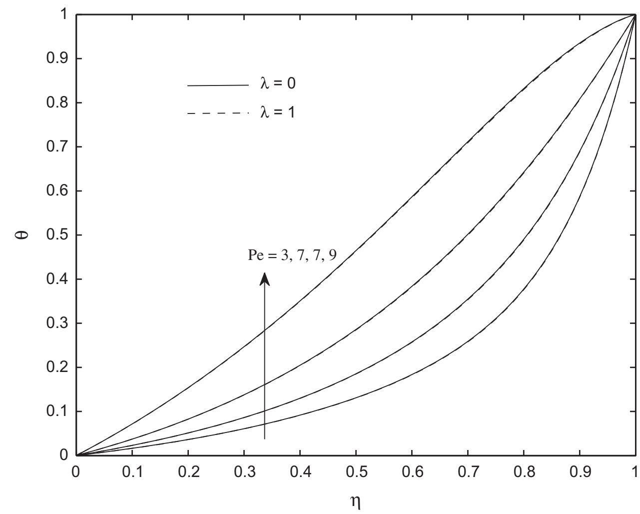

Figure 8 Temperature profiles for different *Pe* when $Br = 1$ and $Re = 2$.

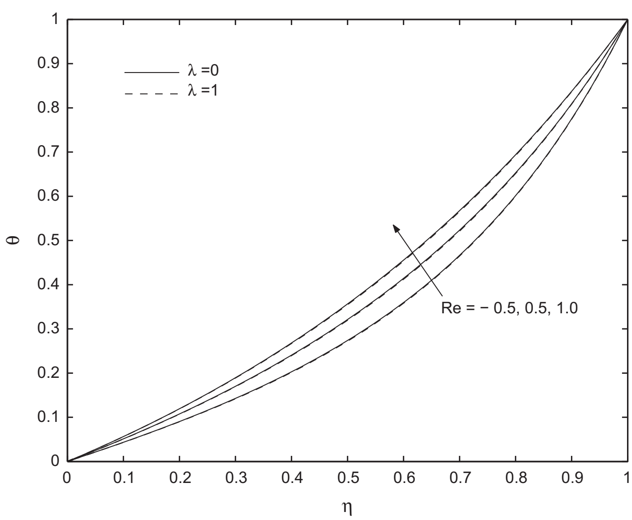

Figure 7 Temperature profiles for different *Re* when $Br = 1$ and $Pe = 3$.

heat transfer take places from fluid to the upper plate, because when there is significant heat generation in the fluid due to viscous and Ohmic dissipations, the temperature of the fluid exceeds the plate temperature which causes heat flow from fluid to the plate.

4. Entropy generation

All thermal systems confront with entropy generation. Entropy generation is squarely associated with thermodynamic irreversibility. It is imperative to determine the rate of entropy generation in a system, in order to optimize energy for efficient operation in the system. The convection process in a channel is inherently irreversible and this causes continuous entropy generation. Woods [41] gave the local volumetric rate of entropy generation for a viscous incompressible conducting fluid in the presence of magnetic field as follows:

$$E_G = \frac{k}{T_0^2}\left(\frac{dT}{dy}\right)^2 + \frac{\mu}{T_0}\left(\frac{du}{dy}\right)^2 + \lambda\frac{\sigma B_0^2}{T_0}u^2. \tag{16}$$

The entropy generation Eq. (16) consists of three terms, the first term is the irreversibility due to the heat transfer, the second term is entropy generation due to viscous dissipation, while the third term is local entropy generation due to the effect of magnetic field (Joule heating or Ohmic heating).

The dimensionless entropy generation number may be defined by the following relationship:

$$N_S = \frac{T_0^2 h^2 E_G}{k(T_h - T_0)^2}. \tag{17}$$

In terms of the dimensionless velocity and temperature, the entropy generation number becomes

$$N_S = \left(\frac{d\theta}{d\eta}\right)^2 + \frac{Br}{\Omega}\left[\left(\frac{du_1}{d\eta}\right)^2 + \lambda M^2 u_1^2\right], \tag{18}$$

where $Br = \frac{\mu_e v_0^2}{k(T_h - T_0)}$ is the Brinkmann number and $\Omega = \frac{T_h - T_0}{T_0}$ the non-dimensional temperature difference.

The entropy generation number N_S can be written as a summation of the entropy generation due to heat transfer denoted by N_1 and the entropy generation due to fluid friction with magnetic field denoted by N_2 given as

$$N_1 = \left(\frac{d\theta}{d\eta}\right)^2, \quad N_2 = \frac{Br}{\Omega}\left[\left(\frac{du_1}{d\eta}\right)^2 + \lambda M^2 u_1^2\right]. \tag{19}$$

In many engineering designs and optimization problems, the contribution of the heat transfer entropy generation to the total entropy generation rate is required therefore; Paoletti et al. [42] presented an alternative irreversibility distribution parameter in terms of Bejan number (*Be*) and defined it as

$$Be = \frac{N_1}{N_S} = \frac{1}{1 + \Phi}, \tag{20}$$

where $\Phi = \frac{N_2}{N_1}$ is the irreversibility ratio. Heat transfer dominates for $0 \leqslant \Phi < 1$ and fluid friction with magnetic effects

Table 1 Rate of heat transfer at the plates $\eta = 0$ and $\eta = 1$ when $Br = 2$, $\beta = 0.1$, $\beta = 0.1$ and $Pe = 3$.

$R \backslash M^2$	$\theta'(0)$				$-\theta'(1)$			
	5	10	15	20	1	10	15	20
0.5	0.51718	0.49732	0.49022	0.48666	2.47588	2.67691	2.72672	2.74821
1.0	0.56581	0.54402	0.53676	0.53316	1.47154	1.63722	1.68494	1.70618
1.5	0.62570	0.60261	0.59522	0.59161	−0.05562	0.08776	0.13426	0.15536
2.0	0.70115	0.67712	0.66964	0.66602	−3.55162	−3.42268	−3.37676	−3.35576

Table 2 Rate of heat transfer at the plates $\eta = 0$ and $\eta = 1$ when $R = 2$, $\beta = 0.1$, $\beta = 0.1$ and $M^2 = 5$.

$Br \backslash Pe$	$\theta'(0)$				$\theta'(1)$			
	4	6	8	10	4	6	8	10
0.2	0.15856	0.06827	0.04072	0.02952	3.06185	5.01396	7.42690	9.33743
0.4	0.24248	0.12164	0.07875	0.05859	2.04908	4.01302	6.85111	8.67440
0.6	0.32641	0.17500	0.11678	0.08765	1.03630	3.01207	6.27532	8.01138
0.8	0.41033	0.22837	0.15481	0.11672	0.02353	2.01113	5.69953	7.34835

Table 3 Rate of heat transfer at the plates $\eta = 0$ and $\eta = 1$ when $R = 2$, $Pe = 3$, $Br = 1$ and $M^2 = 5$.

$\beta_1 \backslash \beta_2$	$\theta'(0)$				$-\theta'(1)$			
	0.2	0.4	0.6	0.8	0.2	0.4	0.6	0.8
0.3	0.69474	0.73451	0.70799	0.70388	4.78096	4.52895	3.48807	3.38299
0.5	0.69193	0.73313	0.70422	0.69986	4.89203	4.70550	3.52113	3.40267
0.7	0.69078	0.73464	0.70336	0.69871	4.97200	4.84169	3.54663	3.41800
0.9	0.69036	0.73721	0.70374	0.69880	5.03228	4.94959	3.56681	3.43020

dominates when $\Phi > 1$. The contribution of both heat transfer and fluid friction to entropy generation are equal when $\Phi = 1$. The Bejan number Be takes the values between 0 and 1 (see [43]). The value of $Be = 1$ is the limit at which the heat transfer irreversibility dominates, $Be = 0$ is the opposite limit at which the irreversibility is dominated by the combined effects of fluid friction and magnetic field and $Be = 0.5$ is the case in which the heat transfer and fluid friction with magnetic field entropy production rates are equal. Further, the behavior of the Bejan number is studied for the optimum values of the parameters at which the entropy generation takes its minimum.

The influences of the different governing parameters on entropy generation within the channel are presented in Figs. 9–20. It is seen from Fig. 9 that the entropy generation number N_S increases with an increase in magnetic parameter

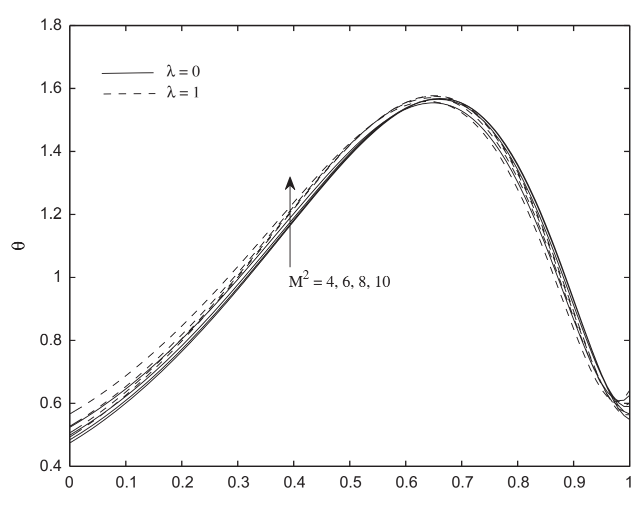

Figure 9 N_S for different M^2 when $Pe = 3$, $\beta_1 = 0.1$, $\beta_2 = 0.1$, $Br = 1$, $Br\Omega^{-1} = 1$ and $Re = 2$.

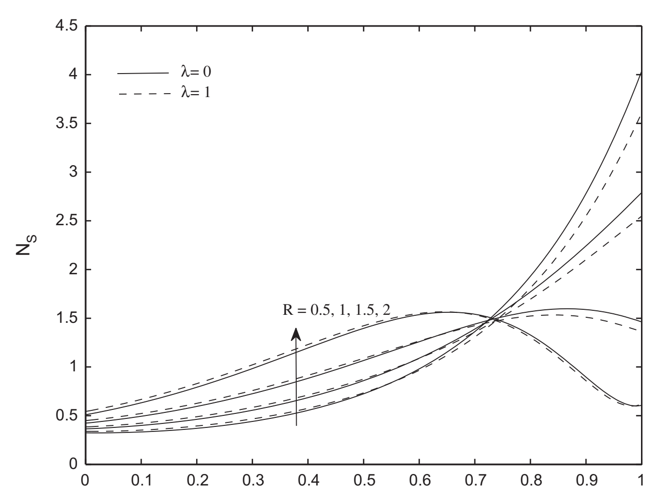

Figure 10 N_S for different Re when $M^2 = 5$, $\beta_1 = 0.1$, $\beta_2 = 0.1$, $Br = 1$, $Pe = 2$ and $Br\Omega^{-1} = 1$.

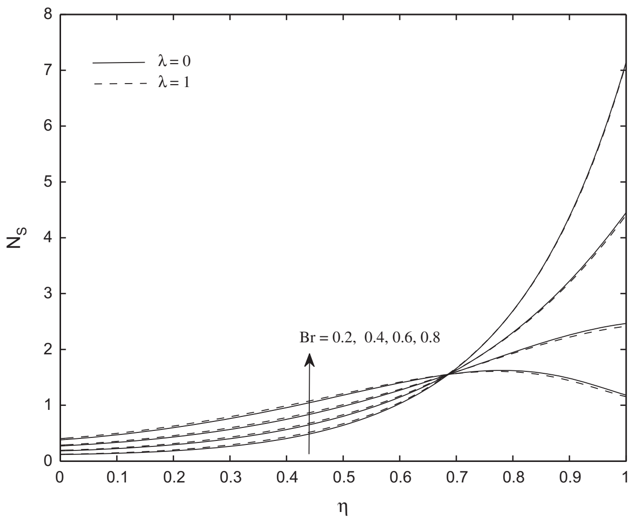

Figure 11 N_S for different Br when $M^2 = 5$, $\beta_1 = 0.1$, $\beta_2 = 0.1$, $Re = 2$, $Pe = 3$ and $Br\Omega^{-1} = 1$.

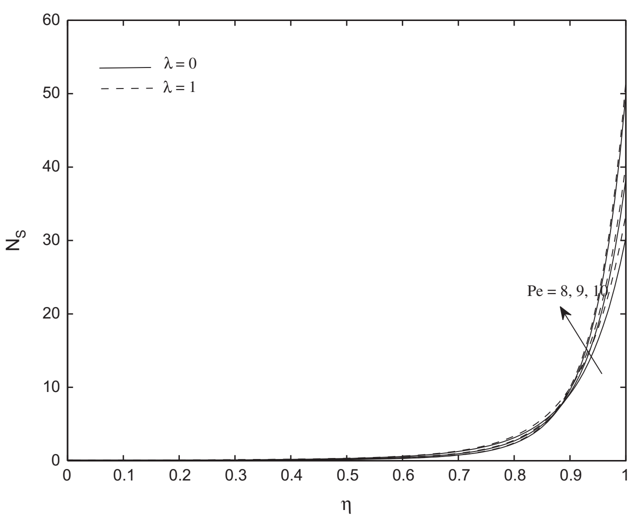

Figure 12 N_S for different Pe when $M^2 = 5$, $\beta_1 = 0.1$, $\beta_2 = 0.1$, $Br = 1$, $Br\Omega^{-1} = 1$ and $R = 2$.

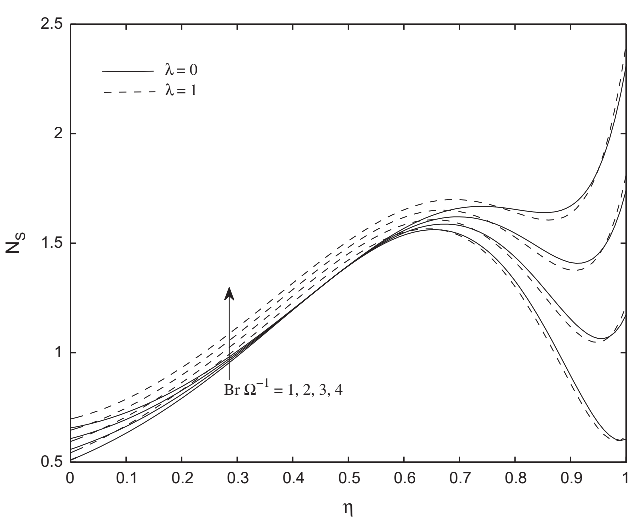

Figure 13 N_S for different $Br\Omega^{-1}$ when $M^2 = 5$, $\beta_1 = 0.1$, $\beta_2 = 0.1$, $Br = 1$, $Pe = 3$ and $R = 2$.

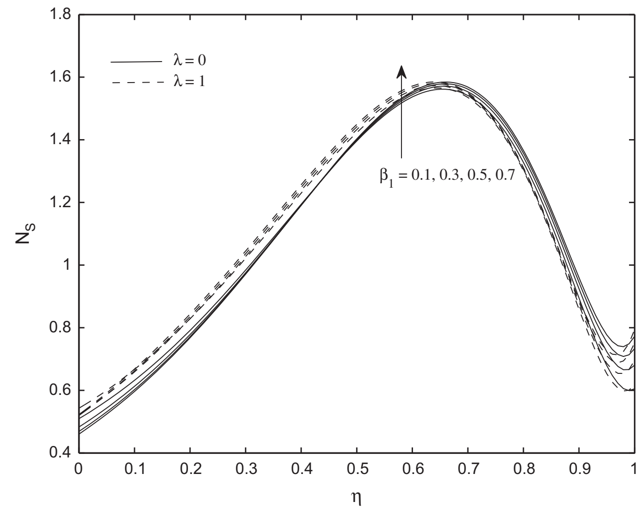

Figure 14 N_S for different β_1 when $M^2 = 5$, $\beta_2 = 0.1$, $Br = 1$, $Pe = 3$, $Br\Omega^{-1} = 1$ and $R = 2$.

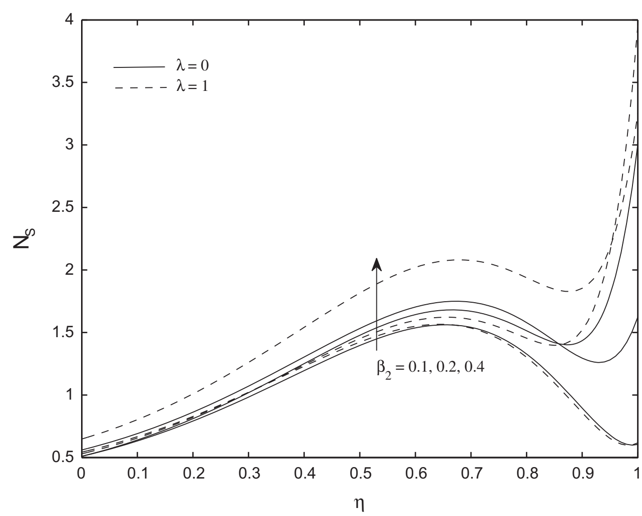

Figure 15 N_S for different β_2 when $M^2 = 5$, $Pe = 2$, $\beta_1 = 0.1$, $Br = 1$, $Br\Omega^{-1} = 1$ and $Re = 2$.

M^2. The effect of magnetic parameter M^2 on the entropy generation number is displayed in Fig. 9. This figure shows that the entropy generation is slightly increases with magnetic parameter M^2. The magnetic parameter M^2 is not too much dominating on entropy generation. A large variation of M^2 causes a small variation in the rate of entropy generation. Fig. 10 show that the entropy generation number N_S increases near the plate $\eta = 0$ and it decreases near the plate $\eta = 1$ with an increase in Reynolds number Re. It is revealed from Fig. 11 that the entropy generation number N_S increases in the region $0 \leqslant \eta \leqslant 0.7$ and it decreases in the region $0.7 < \eta \leqslant 1$ with an increase in Brinkmann number Br. This is physically true since Br is the coefficient of the viscous and Joule dissipations in the energy equation (see Eq. (6)) and its increase raises the fluid temperature via the increase in viscous and Joule dissipations. As the fluid temperature increases, temperature gradient

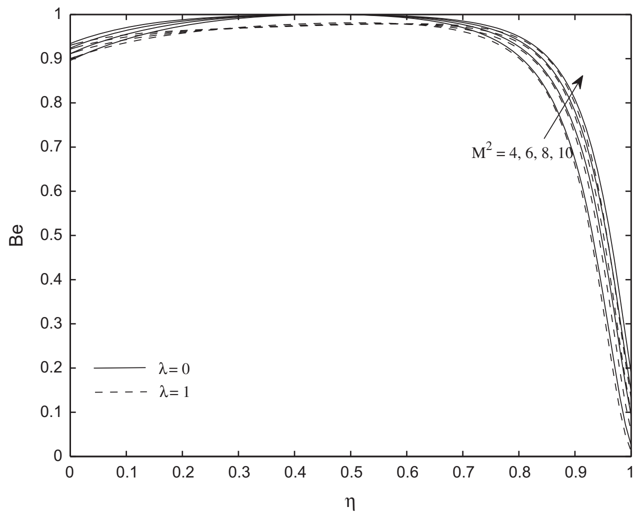

Figure 16 Bejan number for different M^2 when $Pe = 3$, $\beta_1 = 0.1$, $\beta_2 = 0.1$, $Br = 1$, $Br\Omega^{-1} = 1$ and $R = 2$.

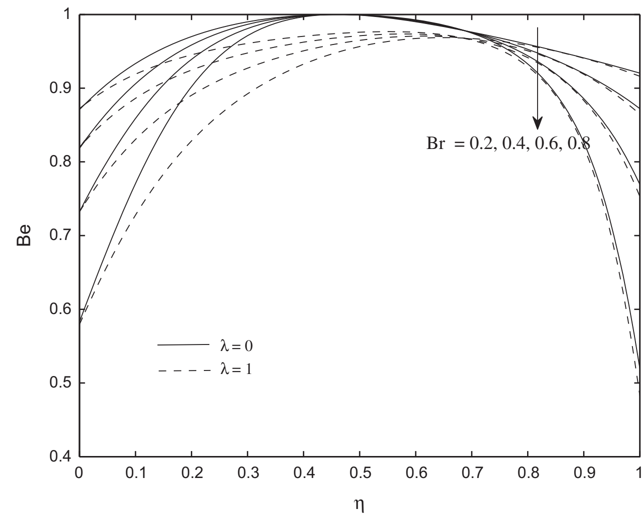

Figure 18 Bejan number for different Br when $M^2 = 5$, $\beta_1 = 0.1$, $\beta_2 = 0.1$, $Pe = 3$ and $Br\Omega^{-1} = 1$.

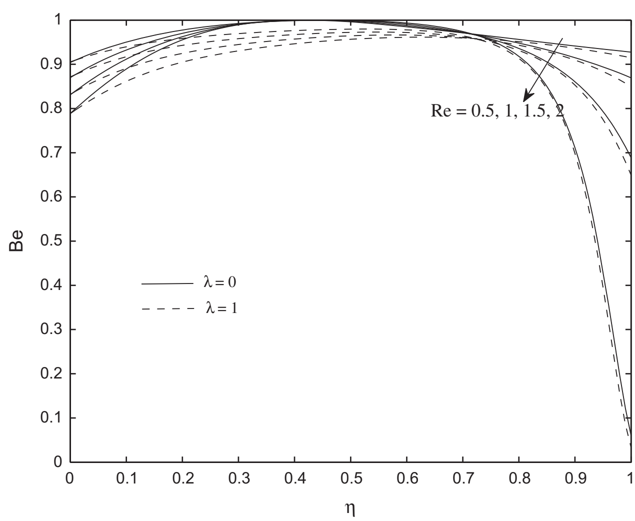

Figure 17 Bejan number for different Re when $M^2 = 5$, $\beta_1 = 0.1$, $\beta_2 = 0.1$, $Br = 1$, $Pe = 3$ and $Br\Omega^{-1} = 1$.

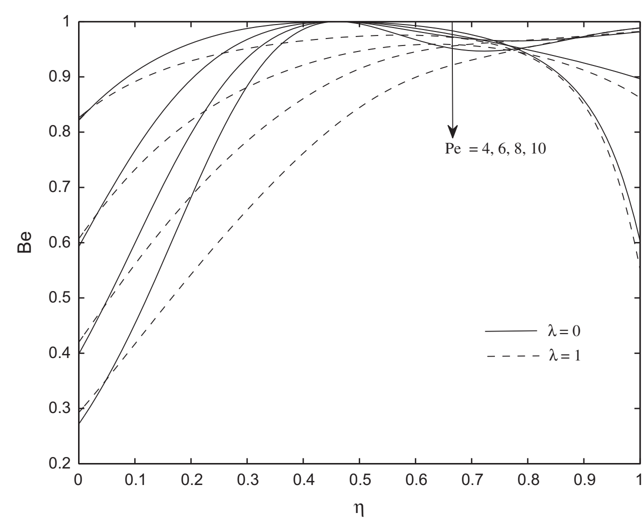

Figure 19 Bejan number for different Pe when $M^2 = 5$, $\beta_1 = 0.1$, $\beta_2 = 0.1$, $Br = 1$, $Br\Omega^{-1} = 1$ and $Re = 2$.

increases within the channel and consequently, there is an increase in entropy generation number in the channel. Figs. 12–15 show that the entropy generation number N_S increases with an increase in either Peclet number Pe or group parameter $Br\Omega^{-1}$ or β_1 or β_2. It is observed that entropy generation number increases with an increase in the group parameter $Br\Omega^{-1}$. This is attributed to the increase in fluid friction irreversibility (N_2) with an increase in $Br\Omega^{-1}$. It is seen from Fig. 16 that the Bejan number Be increases with an increase in magnetic parameter M^2. The effect of magnetic parameter M^2 on the entropy generation number is displayed in Fig. 16. This figure shows that the entropy generation is slightly increases with magnetic parameter M^2. The magnetic parameter M^2 is not too much dominating on entropy generation. A large variation of M^2 causes a small variation in the rate of entropy generation. Figs. 17 and 18 show that the Bejan number Be increases near the plate $\eta = 0$ and it decreases near the plate $\eta = 1$ with an increase in either Reynolds number Re or Brinkmann number Br. An increase in Brinkman number increases the fluid temperature (Fig. 7) as well as temperature gradient within the channel. Consequently, as shown in Fig. 18, the dominance of fluid friction irreversibility over heat transfer irreversibility decreases with increase in Br. Figs. 19–22 reveal that the Bejan number Be increases with an increase in either Peclet number Pe or group parameter $Br\Omega^{-1}$ or β_1. The group parameter is an important dimensionless number for irreversibility analysis. It determines the relative importance of viscous effects to that of temperature gradient entropy generation. It is seen from Fig. 22 that the Bejan number Be increases with an increase in β_2.

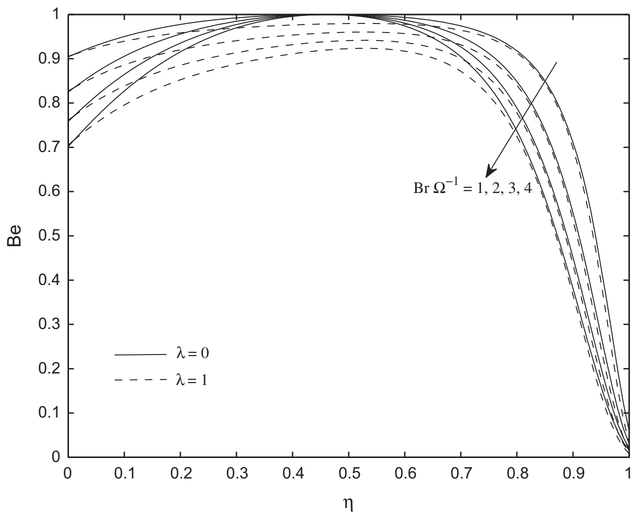

Figure 20 Bejan number for different $Br\Omega^{-1}$ when $M^2 = 5$, $\beta_1 = 0.1$, $\beta_2 = 0.1$, $Br = 1$, $Pe = 3$ and $Re = 2$.

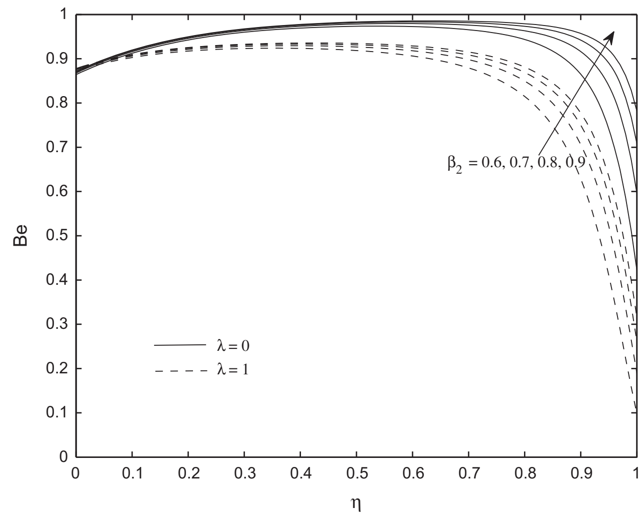

Figure 22 Bejan number for different β_2 when $M^2 = 5$, $\beta_1 = 0.1$, $Br = 1$, $Pe = 3$, $Br\Omega^{-1} = 1$ and $Re = 2$.

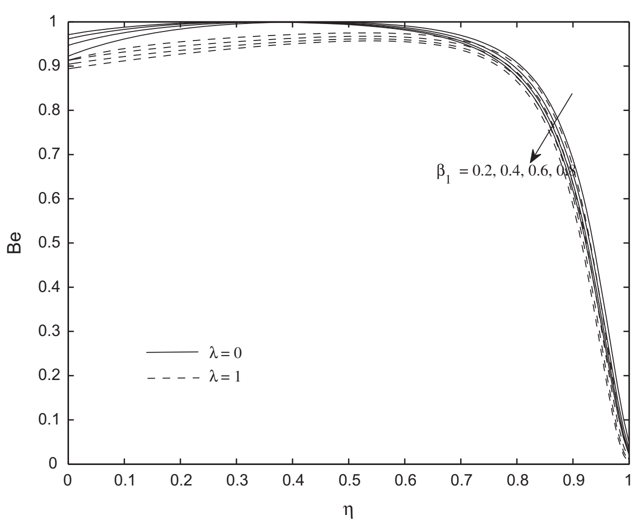

Figure 21 Bejan number for different β_1 when $M^2 = 5$, $\beta_2 = 0.1$, $Br = 1$, $Pe = 3$, $Br\Omega^{-1} = 1$ and $Re = 2$.

5. Conclusion

The combined effects of magnetic field, suction/injection and Navier slip on the entropy generation in an MHD flow through a porous channel with have been investigated. The analytical results obtained for the velocity and temperature profiles are used in order to obtain the entropy generation production. The non-dimensional entropy generation number and the Bejan number are calculated for the problem involved. It is found that, the entropy generation increases with an increase magnetic parameter or group parameter or slip parameter. The rate of heat transfer at the lower plate decreases with an increase in either magnetic parameter or Peclet number. On the other hand, the rate of heat transfer at the upper plate increases with an increase in either Reynolds number or Brinkmann number or slip parameters. It is important to note that the fluid velocity, the fluid temperature as well as entropy generation are significantly influenced by Jule dissipation. The heat transfer irreversibility dominates the flow process within the channel centerline region, while the influence of fluid friction irreversibility can be observed at the channel walls. It is expected that the entropy optimization helps practicing engineers to design thermal systems with lesser energy losses and consequently maximum possible energy available for use.

Acknowledgements

Authors are highly grateful to referees for providing useful suggestions which helped us to modify this research paper.

References

[1] Navier CLMH. Memoire sur les lois du mouvement des fluides. Mem Acad R Sci Paris 1823;6:389–416.
[2] Sahraoui M, Kaviany M. Slip and no-slip temperature boundary conditions at the interface of porous, plane media: convection. Int J Heat Transfer 1994;37(6):1029–44.
[3] Buckingham R, Shearer M, Bertozzi A. Thin film travelling waves and the Navier slip condition. SIAM J Appl Maths 2003;63(2):722–44.
[4] Berh M. On the application of slip boundary condition on curve boundaries. Int J Numer Methods Fluid 2004;45:43–51.
[5] Raoufpanah A. Effects of slip condition on the characteristics of flow in ice melting process. Int J Eng 2005;18(3):1–9.
[6] Chauhan DS, Kumar V. Effect of slip condition on forced convection and entropy generation in a circular channel occupied by highly porous medium: darcy extended Brinkmann–Forchheimer model. Turkish J Eng Environ Sci 2009;33:91–104.
[7] Tripathi D, Gupta PK, Das S. Influence of slip condition on peristaltic transport of a viscoelastic fluid with fractional Burgens model. Therm Sci 2011;15(2):501–15.
[8] Gupta M. Effect of wall slip on the flow in a flat Die for sheet extrusion. ANTEC 2011:1191–6.
[9] Makinde OD, Osalusi E. MHD steady flow in a channel with slip at the permeable boundaries. Rom J Phys 2006;51:319–28.

[10] Khaled ARA, Vafai K. The effect of the slip condition on stokes and couette flows due to an oscillatory wall: exact solutions. Int J NonLin Mech 2004;39:795–809.
[11] Watanebe K, Yanuar MH. Slip of Newtonian fluids at solid boundary. J Jpn Soc Mech Eng 1998;B41:525.
[12] Chen S, Tian Z. Entropy generation analysis of thermal micro-Couette flows in slip regime. Int J Therm Sci 2010;49:2211–21.
[13] Bejan A. Second law analysis in heat transfer. Energy Int J 1980;5:721–32.
[14] Bejan A. Entropy generation through heat and fluid flow. Canada: Wiley; 1994, p. 98.
[15] Bejan A. Second-law analysis in heat transfer and thermal design. Adv Heat Transf 1982;15:1–58.
[16] Bejan A. Entropy generation minimization. New York, NY, USA: CRC Press; 1996.
[17] Bejan A. A study of entropy generation in fundamental convective heat transfer. J Heat Transf 1979;101:718–25.
[18] Bejan A, Tsatsaronis G, Moran M. Thermal design and optimization. New York, NY, USA: Wiley; 1996.
[19] Arpaci VS, Selamet A. Entropy production in flames. Combust Flame 1988;73:254–9.
[20] Arpaci VS, Selamet A. Entropy production in boundary layers. J Thermophys Heat Transf 1990;4:404–7.
[21] Arpaci VS. Radiative entropy production-heat lost to entropy. Adv Heat Transf 1991;21:239–76.
[22] Arpaci VS. Thermal deformation: from thermodynamics to heat transfer. J Heat Transf 2001;123:821–6.
[23] Arpaci VS, Esmaeeli A. Radiative deformation. J Appl Phys 2000;87:3093–100.
[24] Magherbi M, Abbassi H, Ben Brahim A. Entropy generation at the onset of natural convection. Int J Heat Mass Transfer 2003;46:3441–50.
[25] Magherbi M, Abbassi H, Hidouri N, Ben Brahim A. Second law analysis in convective heat and mass transfer. Entropy 2006;8:1–17.
[26] Abbassi H, Magherbi M, Ben Brahim A. Entropy generation in Poiseuille–Benard channel flow. Int J Therm Sci 2003;42:1081–8.
[27] Salas S, Cuevas S, Haro ML. Entropy generation analysis of magnetohydrodynamic inductiondevices. J Phys D: Appl Phys 1999;32:2605–8.
[28] Mahmud S, Tasnim SH, Mamun HAA. Thermodynamics analysis of mixed convection in a channel with transverse hydromagnetic effect. Int J Therm Sci 2003;42:731–40.
[29] Mahmud S, Fraser RA. Flow, thermal and entropy generation characteristic inside a porous channel with viscous dissipation. Int J Therm Sci 2005;44:21–32.
[30] Chauhan DS, Kumar V. Heat transfer and entropy generation during compressible fluid flow in a channel partially filled with porous medium. Int J Energy Tech 2011;3:1–10.
[31] Tasnim SH, Mahmud S, Mamun MAH. Entropy generation in a porous channel with hydromagnetic effects. Exergy 2002;2:300–8.
[32] Eegunjobi AS, Makinde OD. Combined effect of buoyancy force and navier slip on entropy generation in a vertical porous channel. Entropy 2012;14:1028–44.
[33] Makinde OD, Osalusi E. Second law analysis of laminar flow in a channel filled with saturated porous media. Entropy 2005;7(2):148–60.
[34] Makinde OD, Maserumule RL. Thermal criticality and entropy analysis for a variable viscosity Couette flow. Phys Scr 2008;78:1–6.
[35] Makinde OD, Osalusi E. Entropy generation in a liquid film falling along an incline porous heated plate. Mech Res Commun 2006;33:692–8.
[36] Cimpean D, Pop I. Parametric analysis of entropy generation in a channel filled with a porous medium, recent researches in applied and computational mathematics. WSEAS ICACM 2011:54–9.
[37] Cimpean D, Pop I. A study of entropy generation minimization in an inclined channel. Wseas Trans Heat Mass Transfer 2011;6(2):31–40.
[38] Jery AE, Hidouri N, Magherbi M, Ben Brahim A. Effect of an external oriented magnetic field on entropy generation in natural convection. Entropy 2010;12:1391–417.
[39] Dwivedi R, Singh SP, Singh BB. Analysis of incompressible viscous laminar flow through a channel filled with porous media. Int J Stab Fluid Mech 2010;1(1):127–34.
[40] Chinyoka T, Makinde OD. Analysis of entropy generation rate in an unsteady porous channel flow with Navier slip and convective cooling. Entropy 2013;15:2081–99.
[41] Woods LC. Thermodynamics of fluid systems. Oxford, UK: Oxford University Press; 1975.
[42] Paoletti S, Rispoli F, Sciubba E. Calculation of exergetic losses in compact heat exchanger passages. ASME AES 1989;10:21–9.
[43] Cimpean D, Lungu N, Pop I. A problem of entropy generation in a channel filled with a porous medium. Creative Math Inf 2008;17:357–62.
[44] Chinyoka T, Makinde OD, Eegunjobi AS. Entropy analysis of unsteady magnetic flow through a porous pipe with buoyancy effects. J Porous Media 2013;16(9):823–36.
[45] Vyas P, Rai A. Entropy regime for radiative MHD couette flow inside a channel with naturally permeable base. Int J Energy Technol 2013;5(19):1–9.

Sanatan Das is an Assistant Professor of the department of Mathematics, University of Gour Banga, Malda 732 103, India. He was formerly a lecturer of the department of Mathematics, Islampur College, Islampur 733 202, India. He had his B.Sc. (Honours) from Midnapore College (1997), M.Sc. in Applied Mathematics from Vidyasagar University (1999) and Ph.D. from Vidyasagar University (2012). His areas of interest include fluid dynamics, magnetohydrodynamics, heat and mass transfer and porous media. He has to his credit 77 research papers in journals of national and international repute and he is the author of several books. Dr. Das has been undertaking various important administrative work of the university at different positions.

Rabindra Nath Jana is a Professor of the department of Applied Mathematics, Vidyasagar University, Midnapore 721 102, India. He was formerly a Lecturer of the department of Mathematics, Kharagpur College, Kharagpur. He had his B.Sc. (Honours) from Kharagpur College (1969), M.Sc. in Applied Mathematics from IIT Kharagpur (1971), DIIT from IIT Kharagpur (1972) and Ph.D. from IIT Kharagpur (1976) . His areas of interest include fluid dynamics, magnetohydrodynamics, heat transfer and porous media. He has to his credit 140 research papers in journals of national and international repute and he is the author of several books. Prof. Jana has been undertaking various important administrative work of the university at different positions.